Asian Journal of Chemistry; Vol. 28, No. 8 (2016), 1841-1847

ASIAN JOURNAL OF CHEMISTRY

http://dx.doi.org/10.14233/ajchem.2016.19887

Synthesis, Characterization, Non-Linear Optical, Molecular Electrostatic Potential and HOMO-LUMO Analysis Using DFT Study of Novel Chiral Symmetric Schiff Bases

KIVILCIM SENDIL[1,*], GÜVENTÜRK UGURLU[2], HALIL ÇALISKAN[1], MUKADDER YILMAZ[1] and ERTAN SAHIN[3]

[1]Department of Chemistry, Faculty of Science, Kafkas Universty, Kars 36100, Turkey
[2]Department of Physics, Faculty of Science, Kafkas Universty, Kars 36100, Turkey
[3]Department of Chemistry, Faculty of Science, Atatürk Universty, Erzurum 25100, Turkey

*Corresponding author: Tel: +90 474 2251097; E-mail: kivilcimsendil@hotmail.com

Received: 3 February 2016; *Accepted*: 28 April 2016; *Published online*: 30 April 2016; AJC-17903

Three new chiral diimine Schiff bases, 5,5'-methylene-*bis*-salicylidene-α-methylbenzylamine (**2**), 5,5'-methylene*bis*(2-((Z)-((1-(4-methoxyphenyl)ethyl)imino)methyl)phenol) (**3**), 5,5'-methylene*bis*(2-((Z)-((3,3-dimethylbutan-2-yl)imino)methyl)phenol) (**4**) including symmetric imine type have been synthesized. The 5,5'-methylene*bis*-salicylaldehyde (**1**) used as the starting material for the obtained Schiff bases was confirmed by single crystal X-ray diffraction. Characterization of novel symmetric diimine Schiff bases have been done by means of elemental analysis, FT-IR, ^{1}H and ^{13}C NMR spectral studies. Theoretical electronic structure calculations of the B3LYP/6-311+g(d,p) level were performed to optimize the molecular geometry. The non-linear optical properties such as dipole moment, polarizability and first order hyperpolarizability of **1**, **2, 3** and **4** were determined. The HOMO and LUMO energy gaps revealed that the energy gaps reflected the chemical activity of the molecules. To obtain chemical reactivity of the molecules, the molecular electrostatic potential surface maps were plotted over the optimized geometry of the molecules.

Keywords: Chiral Schiff bases, X-ray diffraction, DFT calculation, NMR, Non-linear optical properties.

INTRODUCTION

Schiff bases, products of the condensation reactions between aldehyde and primary amines, were first described by Hugo Schiff in the 19th century [1]. Schiff bases are some of the most widely used organic compounds. They are used as pigments and dyes, catalysts, intermediates in organic synthesis and as polymer stabilizers [2]. Schiff bases have been shown to exhibit a broad range of biological activities, including antifungal, antibacterial, antimalarial, antiproliferative, anti-inflammatory, antiviral and antipyretic [2,3]. Schiff bases have also been employed as ligands for complexation of metal ions [4-7]. Schiff bases play important roles in ring closing reactions [8] and in obtaining the β-lactam antibiotics as a result of cycloaddition with ketene [9].

Chirality plays important roles in diverse fields such as asymmetric catalysis, biological systems, chiral drugs and supramolecular chemistry. Chiral organic compounds are of considerable interests due to their important applications in the probe of chiral structure for biological systems, preparation of chiral catalysts, syntheses of chiral drug and development of multifunctional materials [10-17]. Although the chiral organic molecules have been known for a long time, the pharmaceutical implications of racemic drugs have only been recognized in the last 20 years [18]. Chiral Schiff bases are being most extensively used as the starting material for the synthesis of a drug. The understanding of molecular geometry, delocalization of charges, reactive electrophilic and nucleophilic sites of the compound is critical in the synthesis of a drug and theoretical and experimental studies are being performed to elucidate these points. Parallel with the development in computational chemistry, density functional theory (DFT) has been used extensively to calculate a wide variety of molecular properties and provided reliable results which are in good agreement with experimental data [19].

Organic compounds with aromatic moieties are generally known to easily transport electrons or charges *via*/among their conjugated segments to perform photoelectric or NLO effects. Currently, the organics with electron-donating and electron-withdrawing groups have been regarded as an interesting kind of NLO compounds that are better than inorganic materials [20,21], wherein, the imine-bridged benzene derivatives have shown high optical non-linearities. As a result, these compounds have attracted considerable attention due to their potential applications in modern technology for the preparation of non-linear optical (NLO) materials.

In this work, three new chiral dimine Schiff bases were synthesized for the first time by using symmetric aldehyde. The structure of this newly synthesized Schiff bases were characterized by FT-IR, ^{1}H NMR and ^{13}C NMR spectral studies. DFT methods were used to perform theoretical calculations certain non-linear optical properties (such as dipole moment, polarizability and first order hyper polarizability) and HOMO-LUMO energy gaps for the **1**,**2, 3** and **4** compounds. Moreover, molecular electrostatic potential (MEP) surface maps were plotted over the optimized geometry to elucidate the reactivity of the molecules. The results are valuable for providing insight into molecular properties of symmetric diimine Schiff bases.

EXPERIMENTAL

The reagent grade chemicals used in synthesis of chiral compounds were purchased from Fluka and Merck chemical companies and were used without further purification. Thin-layer chromatography was performed on Merck silica gel 60F254 plates. The elemental analyses (C, H, N) were performed by using Leco 932 model elemental analyzer.^{1}H NMR and^{13}C NMR spectra were recorded on Varian Mercury 400 MHz NMR ultra shield spectrometer using $CDCl_3$ as solvent and Me_4Si as an internal standard. FTIR (KBr pellet, 4000-400 cm^{-1}) spectra were obtained using Mattson 1000 FT-IR spectrophotometer.

All the present calculations have been performed by using DFT method with B3LYP functional [22], where the 6-311+G(d,p) basis set was employed. The non-linear optical properties such as dipole moment, polarizability and first order hyperpolarizability of Schiff bases were computed with the aid of B3LYP/6-311+G(d,p) level of DFT and HF theory. The frontier molecular energies, energy gaps between various occupied and unoccupied molecular orbitals and molecular electrostatic potential (MEP) surface maps of Schiff bases were also calculated with the same method.

X-ray diffraction data of 5,5'-methylene*bis*-salicylaldehyde: For the crystal structure determination, the single-crystal of the 5,5'-methylene*bis*-salicylaldehyde (**1**) was used for data collection on a Rigaku R-AXIS RAPID-S imaging plate diffractometer. The graphite-monochromatized MoK_α radiation (λ = 0.71073 Å) and oscillation scans technique with $\Delta\omega = 5°$ for one image were used for data collection. The lattice parameters were determined by the least-squares methods on the basis of all reflections with $F^2 > 2\sigma(F^2)$. Integration of the intensities, correction for Lorentz and polarization effects and cell refinement was performed using Crystal-clear software [23]. The structures were solved by direct methods using SHELXS-97 and refined by a full-matrix least-squares procedure using the program SHELXL-97 [24]. Crystallographic data for the structures reported in this paper have been deposited with the Cambridge Crystallographic Data Centre as supplementary publication number CCDC 912921. Copies of the data can be obtained free of charge on application to CCDC 12 Union Road, Cambridge CB21 EZ, UK (fax: +44 1223 336 033; e-mail: data_request@ccdc.cam.ac.uk).

General method for the synthesis of chiral symmetric Schiff bases

5,5'-Methylene*bis*(2-((Z)-((1-phenylethyl)imino)-methyl)phenol) (2): 5,5'-Methylene*bis*-salicylaldehyde (**1**) was prepared by the reported method [25]. 5'5-Methylene*bis*-salicylaldehyde (3.36 mmol, 0.84 g) was dissolved in 10 mL ethanol and optically active α-methylbenzlyamine (7.72 mmol) in ethanol was added drop-wise. 2-3 drops of concentrated sulfuric acid was added to the reaction environment and the reaction was refluxed for 2-3 h and filtered. The solution was purified by column chromatography(silica gel/hexane-EtOAc 4:1).5,5'-methylene*bis*(2-((Z)-((1-phenylethyl)imino)-methyl)phenol) (**2**) Schiff base was obtained with 89 % yield. IR (KBr, ν_{max}, cm^{-1}): 3433 (O-H), 1635 (C=C), 1580 (C=N); ^{1}H NMR ($CDCl_3$) δ ppm: 13.41 (broad s, 2H, -OH), 8.34 (s, 2H, -HC=N), 6.90-7.38 (m, 16H, aromatic proton), 4.51 (q, -CH), 3.86 (s, $-CH_2$), 1.62 (d, $-CH_3$); ^{13}C NMR ($CDCl_3$) δ ppm: 163.6 (olefenic -C=N), 117.3-159.7 (aromatic), 68.8 (-C-N), 40.0 ($-CH_2$), 25.1 ($-CH_3$); Elemental analysis (%): Calc.: C, 80.49, H, 6.54, N, 6.06; found: C, 80.35, H, 6.49, N, 6.01 for $C_{31}H_{30}N_2O_2$.

5,5'-Methylene*bis*[2-{(Z)-((1-(4-methoxyphenyl)-ethyl)imino)methyl}phenol] (3): 5'5-Methylene*bis*-salicylaldehyde (3.36 mmol, 0.84 g) was dissolved in 10 mL ethanol and optically active 4-methoxy-α-methylbenzlyamine (7.72 mmol) in ethanol was added drop-wise. 2-3 drops of concentrated sulfuric acid was added to the reaction environment and the reaction was refluxed for 2-3 h and filtered. The solution was purified by column chromatography (silica gel/hexane-EtOAc 4:1). 5,5'-Methylene*bis*(2-((Z)-((1-(4-methoxyphenyl)ethyl)imino)methyl)phenol) (3) Schiff base was obtained with 90 % yield. IR (KBr, ν_{max}, cm^{-1}): 3400 (O-H), 1605 (C=C), 1585 (C=N); ^{1}H NMR ($CDCl_3$) δ ppm: 13.70 (broad s, 2H, -OH), 8.81 (s, 2H, -HC=N), 6.98-7.32 (m, 16H, aromatic proton), 4.40 (m, 1H, CH), 3.88 (s, 2H, $-CH_2$), 3.80 (s,3H, OCH_3), 1.63 (d, $-CH_3$); ^{13}C NMR ($CDCl_3$) δ ppm: 163.5 (olefenic -C=N), 114.4-159.8 (aromatic), 68.8 (-C-N), 55.5 ($O-CH_3$), 40.0 ($-CH_2$), 20.1 ($-CH_3$); Elemental analysis (%): Calc.: C, 75.84, H, 6.56, N, 5.36; found: C, 75.95, H, 6.58, N, 5.41 % for $C_{33}H_{34}N_2O_4$.

5,5'-Methylene*bis*(2-((Z)-((3,3-dimethylbutan-2-yl)-imino)methyl)phenol) (4): 5'5-Methylene*bis*-salicylaldehyde (3.36 mmol, 0.84 g) was dissolved in 10 mL ethanol and optically active 3,3-dimethyl-2-butylamine (7.72 mmol) in ethanol was added drop-wise. 2-3 drops of concentrated sulfuric acid was added to the reaction environment and the reaction was refluxed for 2-3 h and filtered. The solution was purified by column chromatography (silica gel/hexane-EtOAc 4:1). 5,5'-Methylene*bis*[2-{(Z)-((3,3-dimethylbutan-2-yl)-imino)methyl}phenol] (**4**) Schiff base was obtained with 72 % yield. IR (KBr, ν_{max}, cm^{-1}): 3428 (O-H), 1650 (C=C), 1585 (C=N); ^{1}H NMR ($CDCl_3$) δ ppm: 13.62 (broad s, 2H, -OH), 8.24 (s, 2H, -HC=N), 6.80-7.14 (m, 16H, aromatic proton), 3.86 (s, $-CH_2$), 3.07 (m, -CH), 0.90-0.92 ($-CH_3$); ^{13}C NMR ($CDCl_3$) δ ppm: 162.9 (olefenic -C=N), 118.8-160.0 (aromatic), 70.8 (-C-N), 34.2 (CH_2), 40.1 ($-CH_2$), 18.7, 19.5, 20.0 ($-CH_3$); Elemental analysis (%): Calc.: C, 76.74, H, 9.06, N, 6.63; found: C, 76.85, H, 9.19, N, 6.58 % for $C_{27}H_{38}N_2O_2$.

RESULTS AND DISCUSSION

Three new chiral diimine Schiff bases including two symmetric imine type have been synthesized. The performed

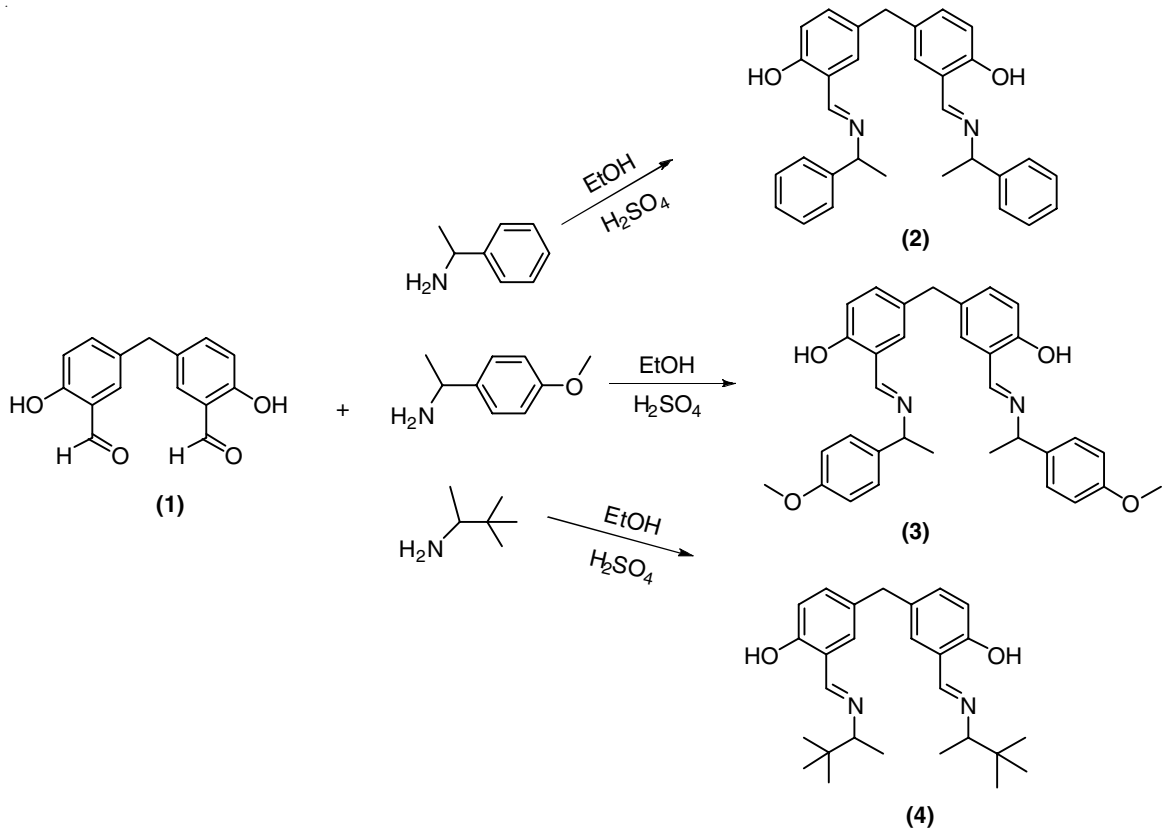

Scheme-I: Schematic representation of the preparation of chiral symetric Schiff bases (**2, 3, 4**) with its chemical diagram

reaction is shown in **Scheme-I**. The 5'5-methylene*bis*-salicylaldehyde (**1**) used as the starting material for the obtained Schiff base was confirmed by single crystal X-ray diffraction.

Description of crystal structure: The crystal structure analysis confirmed the structure of compound **1** as 5,5'-methylene-*bis*-salicylaldehyde (Fig. 1). Hydrogens attached to carbon and oxygen atoms were positioned geometrically and refined using a riding model. The details of the final refinements are given in Table-1. The crystal structure and the crystal packing fragment for compound **1** are shown in Figs. 1 and 2.

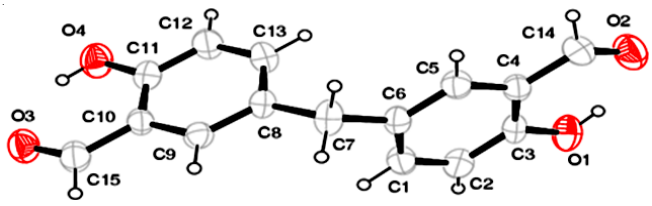

Fig. 1. Crystal structure of 5,5'-methylene*bis*-salicylaldehyde (**1**) compound

In the structure, O-C bond lengths are in the range of 1.224(6)-1.365(5) Å. C-C, C-H and O-H bond lengths are in the expected range. O-C-C bond angles are 117.8(4)° and 123.7(4)°. C6-C7-C8 bond angle is 112.7(4)° and phenyl rings with the substituted units are significantly twisted relative to each other [dihedral angle formed by LSQ-planes is 86.20(9)°].

Some of the selected experimental bond lengths and bond angles are shown in Table-2 in comparison with the calculated values by HF and B3LYP/6-311+g(d,p) levels. As shown in Table-2, theoretically calculated bond lengths and bond angles are in reasonable agreement with the crystallographic data.

TABLE-1
CRYSTAL DATA AND STRUCTURE REFINEMENT FOR COMPOUND **1**

Empirical formula	$C_{15}H_{12}O_4$
Formula weight	356.3
Temperature	293(2) K
Wavelength	0.71073 Å
Crystal system	Monoclinic
Space group	$P2_1/n$
Unit cell dimensions	a = 7.8156(5) Å; α = 90°
	b =11.7496(8) Å ; β = 94.660(4)°
	c =13.2532(9) Å ; γ = 90°
Volume	1213.02(14) $Å^3$
Z	4
Density (calculated)	1.403 g/c m^3
Absorption coefficient	0.102 mm^{-1}
F(000)	536
Crystal size	0.20 mm × 0.02 mm × 0.02 mm
θ range for data collection	2.3-26.4°
Index ranges	$-9 \le h \le 9, -13 \le k \le 14, -16 \le l \le 16$
Reflections collected	16946
Independent reflections	2492 [R_{int} = 0.106]
Completeness to θ = 26.4°	99.9 %
Max. and min. transmission	0.990 and 0.976
Refinement method	Full-matrix least-squares on F^2
Data/restraints/parameters	1058/0/178
Goodness-of-fit on F^2	1.036
Final R indices [$F^2 > 2\sigma(F^2)$]	R1 = 0.071; wR2 = 0.147
Rindices (alldata)	R1 = 0.167; wR2 = 0.194
Largest diff. peak and hole	0.143 and –0.200 e $Å^{-3}$

In the crystal, molecules are linked *via* intramolecular O-H···O hydrogen bonds resulting in the formation of a dimeric structure lying parallel to the bc plane (Fig. 2). Intra- and inter-molecular hydrogen bonds are shown as dashed lines in Table-3.

TABLE-2
OPTIMIZED GEOMETRICAL PARAMETERS OF 5,5'-METHYLENE*BIS*-SALICYLALDEHYDE BY HF AND B3LYP/6-311+g(d,p)

Parameter	Methods		Exp.	Parameter	Methods		Exp.
	HF	B3LYP/6-311+g(d,p)			HF	B3LYP/6-311+g(d,p)	
Bond length (Å)				Bond angle (°)			
O1-C3	1.348	1.365	1.363	C5-C6-C7	121.37	121.23	122.8
O4-C11	1.348	1.366	1.360	C1-C6-C7	121.26	121.10	120.3
C6-C5	1.378	1.388	1.364	C9-C8-C13	117.37	177.61	116.6
C1-C6	1.395	1.403	1.393	C4-C3-O1	118.68	118.40	121.3
C8-C27	1.518	1.519	1.512	C4-C3-C2	119.66	119.68	120.7
C3-C4	1.387	1.404	1.396	C3-C4-C14	121.28	121.42	121.2
C5-C4	1.395	1.403	1.404	C6-C5-C4	122.21	122.23	122.6
C10-C9	1.388	1.399	1.405	C6-C7-C8	114.98	115.06	112.7
C10-C11	1.394	1.407	1.387	C9-C10-C11	119.19	118.99	118.9
C13-C12	1.385	1.391	1.382	C11-C10-C15	121.10	121.23	121.8
O3-C15	1.187	1.214	1.237	O4-C11-C10	118.33	118.21	122.3
O2-C14	1.188	1.214	1.224	C5-C6-C1	117.40	117.65	116.9
C6-C7	1.518	1.519	1.512	C9-C8-C7	121.42	121.35	122.5
C9-C8	1.386	1.393	1.380	C13-C8-C7	121.19	121.01	120.9
C8-C13	1.388	1.400	1.387	O1-C3-C2	121.65	121.91	118.1
C3-C2	1.390	1.397	1.371	C3-C4-C5	119.06	118.84	118.1
C4-C14	1.484	1.480	1.437	C5-C4-C14	119.64	119.72	120.7
C2-C1	1.377	1.388	1.380	C8-C9-C10	122.10	122.11	122.3
C10-C15	1.486	1.482	1.454	C1-C2-C3	119.97	120.12	119.0
C12-C11	1.383	1.394	1.374	C9-C10-C15	119.70	119.77	119.3
				C8-C13-C12	121.82	121.61	122.6
				O4-C11-C12	121.99	122.09	117.8

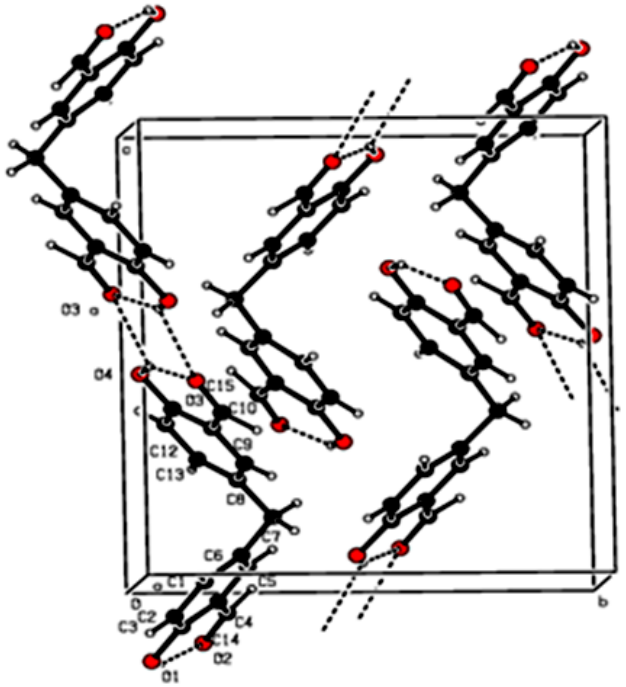

Fig. 2. A view along the *c*-axis of the crystal packing of (**1**) compound

TABLE-3
HYDROGEN BONDS FOR COMPOUND **1**

D–H···A	D–H	H···A	D···A	D–H···A
O(1)–H(1O) ···O(2)	0.82	1.89	2.608(4)	146
O(4)–H(4O) ···O(3)	0.82	1.94	2.650(4)	145
O(4)–H(4O) ···O(3)[a]	0.82	2.57	3.087(4)	123
Symmetry code: (a) 3-x, -y, 1-z				

Geometries of the Schiff bases were optimized in the gas phases. The optimized structure of the **1, 2, 3** and **4** species with labeling of their atoms are shown in Figs. 1 and 3.

Non-linear optical effects (NLO): Non-linear optical (NLO) effects arise from the interactions of electromagnetic fields in various media to produce new fields altered in phase, frequency, amplitude or other propagation characteristics from the incident fields [26]. Non-linear optical is at the fore-front of current research because of its importance in providing the key functions of frequency shifting, optical modulation, optical switching, optical logic and optical memory for the emerging technologies in areas such as telecommunications, signal processing and optical interconnections [27-30]. Organic molecules with significant non-linear optical activity generally consist of a π-electron conjugated moiety substituted by an electron donor group on one end of the conjugated structure and an electron acceptor group on the other end, forming a 'push-pull' conjugated structure [31].

The total static dipole moment (μ), linear polarizability (α) and the first hyper polarizability (β) using the x, y, z components are defined as [32,33]:

$$\mu = \left(\mu_x^2 + \mu_y^2 + \mu_z^2\right)^{1/2}$$

$$\alpha = \frac{1}{3}\left(\alpha_{xx} + \alpha_{yy} + \alpha_{zz}\right)$$

$$\beta = \sqrt{\left(\beta_{xxx} + \beta_{yyy} + \beta_{zzz}\right)^2 + \left(\beta_{yyy} + \beta_{xxy} + \beta_{yzz}\right)^2 + \left(\beta_{zzz} + \beta_{xxz} + \beta_{yyz}\right)^2}$$

The dipole moments (μ), linear polarizability (α) and first order hyper polarizabilities (β) were calculated using different basis sets at the HF and DFT (B3LYP/6-311+g(d,p) of **1**, **2, 3** and **4** molecules as given in Table-4. Since the values of polarizability (α) and hyper polarizability (β) of the Gaussian 09 output are reported in atomic units (a.u.), the calculated values have been converted into electrostatic units (e.s.u.) (1 a.u.= 8.639 10^{-33} e.s.u.). Urea is one of the prototypical

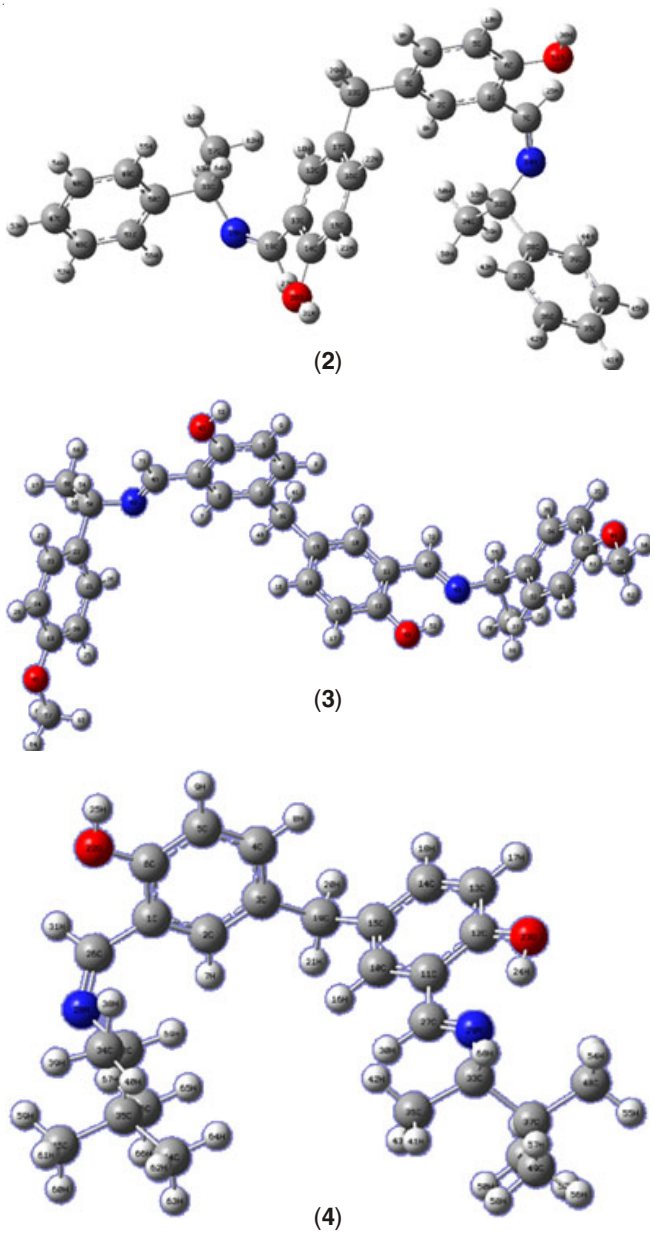

Fig. 3. B3LYP optimized geometries of the (**2**), (**3**), (**4**) chiral symmetric Schiff bases

molecules used in the study of the NLO properties of molecular systems. Therefore, it is used frequently as a threshold value for comparative purposes. The calculated values of **1, 2, 3** and **4** compounds given in Table-4 are greater than those reported for urea [34]. These results indicate that **1, 2, 3** and **4** compounds are good candidate of non-linear optical material.

When we look at the values obtained for the first hyper polarizability, it is clearly seen that this electric property has a strong dependence on the basis sets used in calculations. It is well known that electron correlation makes large contributions to the calculated hyper polarizability. Hence, to calculate the hyper polarizability tensor components accurately it is very necessary to take the electron correlation effect into account.

HOMO and LUMO analyses: The interaction of a molecule with other species is determined by the HOMO and LUMO molecular orbitals, called frontier orbitals. Determination of frontier orbital energies is important to characterize the chemical reactivity and kinetic stability of the molecule. A molecule with a small frontier orbital gap is more polarizable and is generally associated with a high chemical reactivity, low kinetic stability and is also termed as soft molecule [35]. The frontier molecular orbitals also play an important role in the electric and optical properties [36,37]. The HOMO represents the ability to donate an electron, LUMO as an electron acceptor represents the ability to obtain an electron.

The HOMO and LUMO energies calculated by HF and B3LYP/6-311+G(d,p) methods. The electronic absorption corresponds to the transitions from the ground to the first excited state and is mainly described by one electron excitation from the HOMO to the LUMO. The energy of the HOMO is directly related to the ionization potential; however, the LUMO energy is directly related to the electron affinity.

The energy gap given as the energy difference between the HOMO and LUMO gives an idea about the stability of the structure. The conjugated molecules are characterized by a small highest occupied molecular orbital-lowest unoccupied molecular orbital (HOMO-LUMO) separation, which is the result of a significant degree of intramolecular charge transfer from the end-capping electron-donor groups to the efficient electron-acceptor groups through π-conjugated path [38,39]. The plots of highest occupied molecular orbitals (HOMOs) and lowest unoccupied molecular orbitals (LUMOs) are shown in Fig. 4.

Molecular electrostatic potential (MEP) maps: The molecular electrostatic potential (MEP) is related to the electronic density and is a very useful descriptor for determining sites for electrophilic and nucleophilic reactions as well as hydrogen-bonding interactions [40-42]. The electrostatic potential V(r) is also well suited for analyzing process based on the 'recognition' of one molecule by another, as in drug-receptor and enzyme-substrate interactions, because it is through their potentials that two species first 'see' each other [43,44]. Being a real physical property, V(r) can be determined experimentally by diffraction or theoretically by computational methods.

To predict reactive sites of electrophilic and nucleophilic attack for the investigated molecule, the MEP at the B3LYP/

TABLE-4
CALCULATED ENERGIES, DIPOLE MOMENT, LINEAR POLARIZABILITY AND FIRST HYPERPOLARIZABILITY OF **1**, **2**, **3** AND **4** COMPOUNDS

Parameter	Compound **1**		Compound **2**		Compound **3**		Compound **4**	
	HF	DFT	HF	DFT	HF	DFT	HF	DFT
μ (D)	8.50	8.30	5.83	5.64	3.17	3.16	1.58	1.54
α (Å^3)	25.6	26.3	53.3	58.3	101.0	212.6	38.5	42.8
β (e.s.u.)	1.3×10^{-30}	$2. \times 10^{-30}$	1.9×10^{-30}	2.7×10^{-30}	3.5×10^{-31}	3.9×10^{-31}	1.3×10^{-30}	2.5×10^{-30}
Electronic energy (a.u.)	-874.6	-879.9	-1450.3	-1459.6	-1677.8	-1688.4	1303.4	1312.0

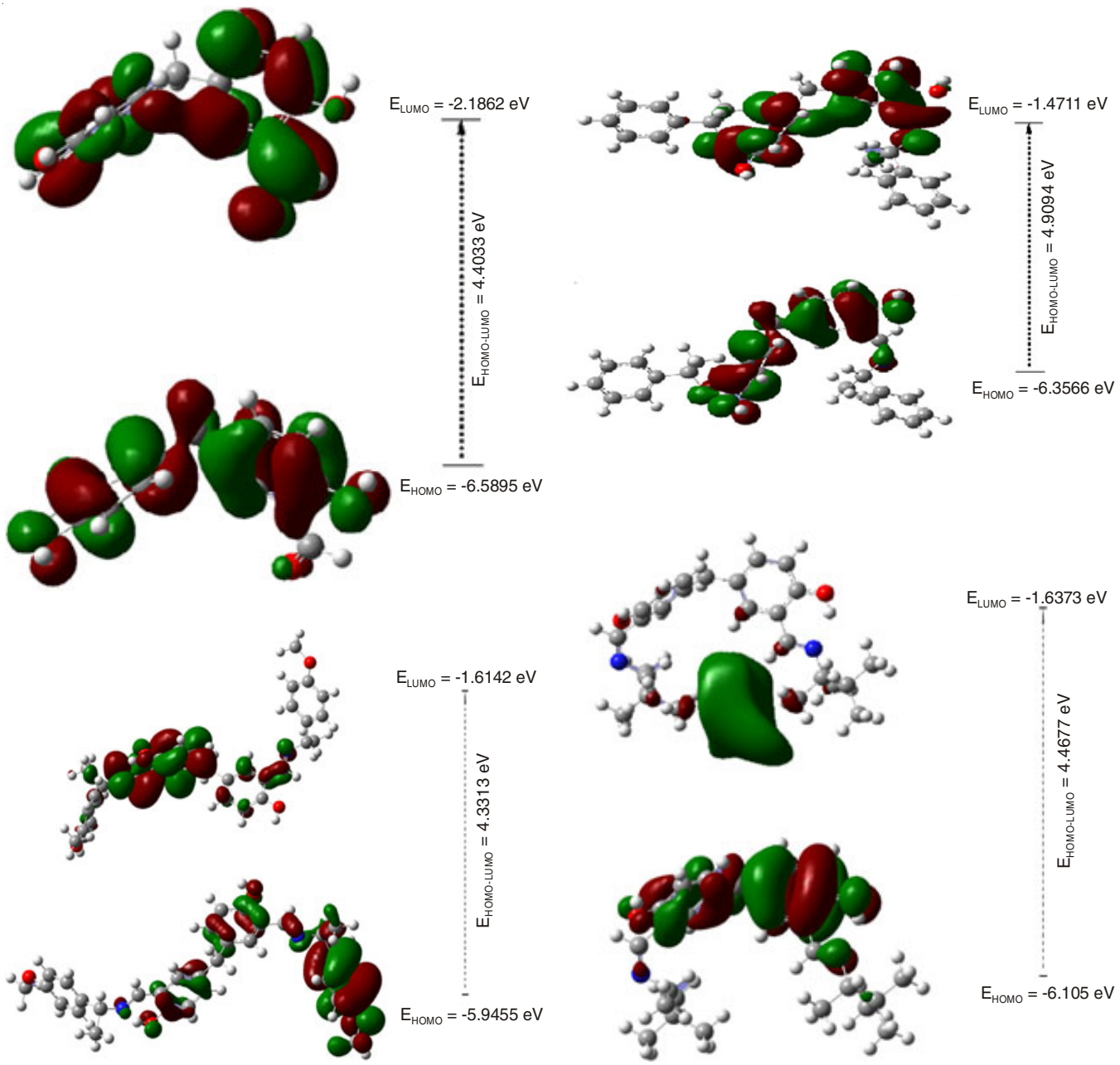

Fig. 4. Frontier orbitals of compounds **1**, **2**, **3**, **4**

6-311+G(d,p) optimized geometry was calculated. The obtained MEP maps are given in Fig. 5 for **1, 2, 3** and **4** molecules, respectively. The different values of the electrostatic potential at the surface are represented by different colours; red represents regions of most electronegative electrostatic potential, blue represents regions of most positive electrostatic potential and green represents regions of zero potential. Potential increases in the order red < orange < yellow < green < blue. The negative (red and yellow) and positive (blue) regions of MEP given in Fig. 5 are related to the electrophilic reactivity and to the nucleophilic reactivity, respectively.

As can be seen from Fig. 5 for **1** compound, negative regions are observed around carbonyl groups while the positive regions are observed around -OH groups. This indicates that the negative regions, *i.e.*, carbonyl groups, are prone to electrophilic attacks while the positive regions, *i.e.*, the -OH groups, are prone to nucleophilic attacks. In the MEP map of the molecule **2, 3, 4** (Fig. 5), the negative regions (yellow) are observed around -C=N groups and in the benzene ring while the positive regions (blue) are observed around the -OH groups. The fact that there is a weak negative region around carbonyl groups and a strong positive region around OH groups, make formation of intramolecular (N….H-O) hydrogen bonding possible between these groups. However, existence of these bonds could check *via* X-ray measurements but we were not able to obtain proper crystal for X-ray measurements from this Schiff base.

ACKNOWLEDGEMENTS

This work was supported by TUBITAK (Project No: 108T982).

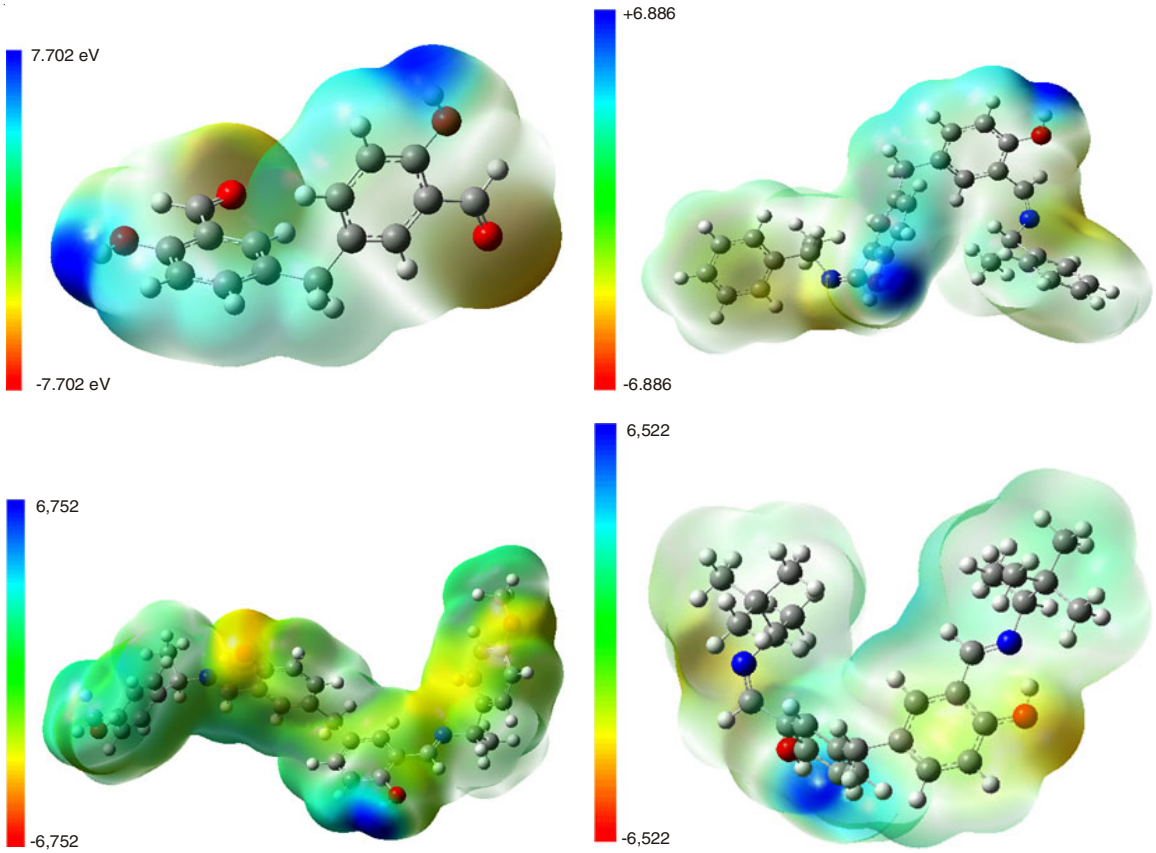

Fig. 5. Molecular electrostatic potential map calculated at B3LYP/6-311+G(d,p) level of **1**, **2, 3** and **4** compounds

REFERENCES

1. H. Schiff, *Justus Liebigs Ann. Chem.*, **150**, 193 (1869).
2. D.N. Dhar and C.L. Taploo, *J. Sci. Ind. Res. (India)*, **41**, 501 (1982).
3. P. Przybylski, A. Huczynski, K. Pyta, B. Brzezinski and F. Bartl, *Curr. Org. Chem.*, **13**, 124 (2009).
4. M.R. Maurya, I. Jain and S.J.J. Titinchi, *Appl. Catal. A*, **249**, 139 (2003).
5. M. Cazacu, M. Marcu, A. Vlad, A. Tóth and C. Racles, *J. Polym. Sci.*, **41**, 3169 (2003).
6. H.L. Siddiqui, A. Iqbal, S. Ahmad and G.W. Weaver, *Molecules*, **11**, 206 (2006).
7. C.A. Sureshan and P.K. Bhattacharya, *Polyhedron*, **16**, 489 (1997).
8. F. Aydogan, N. Öcal, Z. Turgut and C. Yolacan, *Bull. Korean Chem. Soc.*, **22**, 476 (2001).
9. J. March, Advanced Organic Chemistry, Wiley, New York (1972).
10. G. Gottarelli, S. Lena, S. Masiero, S. Pieraccini and G.P. Spada, *Chirality*, **20**, 471 (2008).
11. K. Szacilowski, W. Macyk, A. Drzewiecka-Matuszek, M. Brindell and G. Stochel, *Chem. Rev.*, **105**, 2647 (2005).
12. D.N. Dybtsev, A.L. Nuzhdin, H. Chun, K.P. Bryliakov, E.P. Talsi, V.P. Fedin and K. Kim, *Angew. Chem. Int. Ed.*, **45**, 916 (2006).
13. Y.H. Liu, X.L. Liu, D.M. Yuan, Y.C. Shi, X.B. Jing and J. Wu, *Chin. J. Org. Chem.*, **25**, 893 (2005).
14. J. Inanaga, H. Furuno and T. Hayano, *Chem. Rev.*, **102**, 2211 (2002).
15. G.C. Fu, *Acc. Chem. Res.*, **39**, 853 (2006).
16. H.C. Aspinall, *Chem. Rev.*, **102**, 1807 (2002).
17. G. Chelucci and R.P. Thummel, *Chem. Rev.*, **102**, 3129 (2002).
18. N.M. Davies and X.W. Teng, *Adv. Pharmacy*, **1**, 242 (2003).
19. W. Koch and M.C. Holthausen, A Chemist's Guide to Density Functional Theory, WILEY/VCH verlagGmbH, Weinheim, edn 2 (2001).
20. H. Ünver, A. Karakas and A. Elmali, *J. Mol. Struct.*, **702**, 49 (2004).
21. R.R.B.N.K. Sethuraman, R.R. Babu, N. Vijayan, R. Gopalakrishnan and P. Ramasamy, *Spectrochim. Acta A*, **66**, 707 (2007).
22. C. Lee, W. Yang and R.G. Parr, *Phys. Rev. B*, **37**, 785 (1988).
23. Rigaku, Crystal-Clear Version 1.3.6, Rigaku American Corporation 9009 New Trails Drive, The Woodlands, TX 77381-5209, USA (2005).
24. G.H. Sheldrick, SHELXS-97 and SHELXS-97, University of Gottingen, Germany (1997).
25. C.S. Marvel and N. Tarkoy, *J. Am. Chem. Soc.*, **79**, 6000 (1957).
26. Y.X. Sun, Q.-L. Hao, W.-X. Wei, Z.-X. Yu, L.-D. Lu, X. Wang and Y.-S. Wang, *J. Mol. Struct. THEOCHEM*, **904**, 74 (2009).
27. C. Andraud, T. Brotin, C. Garcia, F. Pelle, P. Goldner, B. Bigot and A. Colle, *J. Am. Chem. Soc.*, **116**, 2094 (1994).
28. V.M. Geskin, C. Lambert and J.L. Bredas, *J. Am. Chem. Soc.*, **125**, 15651 (2003).
29. M. Nakano, H. Fujita, M. Takahata and K. Yamaguchi, *J. Am. Chem. Soc.*, **124**, 9648 (2002).
30. D. Sajan, H. Joe, V.S. Jayakumar and J. Zaleski, *J. Mol. Struct.*, **785**, 43 (2006).
31. D. Sajan, J. Binoy, I. Hubert Joe, V.S. Jayakumar and J. Zaleski, *J. Raman Spectrosc.*, **36**, 221 (2005).
32. H. Petek, C. Albayrak, E. Agar and H. Kalkan, *Acta Crystallogr.*, **E62**, 3685 (2006).
33. H. Tanak, *J. Mol. Struct. THEOCHEM*, **950**, 5 (2010).
34. H. Tanak, A.A. Agar and O. Büyükgüngör, *Spectrochim. Acta A*, **87**, 15 (2012).
35. I. Fleming, Frontier Orbitals and Organic Chemical Reactions, John Wiley & Sons, New York (1976).
36. T. Karakurt, M. Dincer, A. Cetin and M. Sekerci, *Spectrochim. Acta A*, **77**, 189 (2010).
37. C.H. Choi and M. Kertesz, *J. Phys. Chem. A*, **101**, 3823 (1997).
38. D.F.V. Lewis, C. Ioannides and D.V. Parke, *Xenobiotica*, **24**, 401 (1994).
39. E. Scrocco and J. Tomasi, *Adv. Quantum Chem.*, **11**, 115 (1978).
40. F.J. Luque, J.M. Lopez and M. Orozco, *Theor. Chem. Acc.*, **103**, 343 (2000).
41. N. Okulik and A.H. Jubert, *Int. Elctron. J. Mol. Des.*, **4**, 17 (2005).
42. P. Politzer, P.R. Laurence and K. Jayasuriya, *Environ. Health Perspect.*, **61**, 191 (1985).
43. E. Scrocco and J. Tomasi, Topics in Current Chemistry, Springer, London (1973).
44. P. Politzer and D.G. Truhlar, Chemical Applications of Atomic and Molecular Electrostatic Potentials, Plenum, New York (1981).